

# On the Persistence of Auxin Patterns with External Forcing

Dillon Chan and Inah Infante

April 15, 2018

# Contents

<b>1</b>	<b>Abstract</b>	<b>3</b>
<b>2</b>	<b>Introduction</b>	<b>3</b>
<b>3</b>	<b>Basic Auxin Flux Model</b>	<b>4</b>
<b>4</b>	<b>Auxin Self-Feedback Model</b>	<b>4</b>
<b>5</b>	<b>Model Extension</b>	<b>5</b>
<b>6</b>	<b>Discussion</b>	<b>7</b>
6.1	Numerical Calculations . . . . .	7
6.2	Extended model results . . . . .	7
6.2.1	Basic Model Extension . . . . .	8
6.2.2	Self-feedback Model Extension . . . . .	8
6.3	High auxin production . . . . .	11
6.4	Spot-like patterns with the Basic Model . . . . .	11
<b>7</b>	<b>Conclusions</b>	<b>13</b>

## 1 Abstract

Auxins are a class of plant hormones present in varying concentration in all parts of the plant. They are essential to regulating plant body development, tissue differentiation, and growth responses to external stimuli. The pattern of auxin distribution within the plant is a key component to these processes. Modelling auxin distribution in plant tissues therefore further our understanding of the inner mechanisms of plant growth and development. Developing mathematical models of plant growth will help researchers test out hypothesis *in silico* and produce more accurate predictions about plant behaviour. This has applications in agriculture, where plant growth can be directed and designed to exhibit certain features that better fulfill our needs.

Auxins are moved from cell to cell by auxin transporters. One of these transporters is a family of proteins called PIN, whose interaction with auxin is important for pattern formation. Building on mathematical models developed by Fujita and Mochizuki (2006) [3] and Hayakawa, Tachikawa, and Mochizuki (2015) [4], we explored different pattern formations of auxin distribution due to external stimuli by adding a forcing function.

## 2 Introduction

The plant hormone auxin controls a variety of important developmental processes. Auxins affect processes from embryogenesis and post embryonic root and shoot development to vascular tissue differentiation and growth responses to external stimuli [7].

Many characteristics of how auxin affects these developmental processes depend on the distribution of auxin concentration within the plant tissue, for example, where it forms local maxima and gradients [1]. There are two types of auxin distribution patterns observed in plant tissues, “spot” patterns and “passage” patterns. In shoot apical meristems, the areas with high auxin concentration give rise to primordia and these areas form spot-like patterns [8]. Additionally, auxins form passage-like patterns in leaves and this influences vascular patterning, e.g. leaf venation [11]. These patterns occur based on the mechanics of directional cell-to-cell auxin transport [7].

In this paper, we focus on PIN-FORMED (PIN), a family of proteins that act as auxin efflux carriers. PIN proteins are asymmetrically localized in plasma membranes and their localization is consistent with the direction of auxin transport. In shoot apical meristems, PIN proteins are found to be localized in the same areas with high auxin concentrations. PIN proteins are also a major component in auxin transportation that results in vascular patterning [1].

### 3 Basic Auxin Flux Model

Fujita and Mochizuki (2006) [3] proposed a mathematical model that makes use of the canalization hypothesis, which assumes a positive feedback effect between auxin flux and PIN orientation. This hypothesis states that PIN is localized in one direction of the cell membrane and auxin flows out of that direction. Once auxin flows out, the flow (or the “flux”) in that direction increases [9].

Fujita and Mochizuki modelled the plant tissue as a two-dimensional arrangement of hexagonal cells, where  $i$  indicates the position of a cell and  $k$  indicates the cell membrane side of the hexagonal cell.

The differential equations for the dynamics of auxin concentration ( $a_i$ ) and that of PIN ( $p_{ik}$ ) are as follows,

$$\begin{aligned} \frac{da_i}{dt} &= 1 - Aa_i - \sum_k f_{ik} \\ \frac{dp_{ik}}{dt} &= B \frac{g(f_{ik})}{\sum_l g(f_{il})} - p_{ik} \\ f_{ik} &= a_i p_{ik} - a_{i'} p_{i'k'} \\ g(f_{ik}) &= \frac{1}{1 + \exp(-\alpha(f_{ik}/f_0 - \beta))} \end{aligned}$$

where  $A$  is the degradation rate of auxin and  $f_{ik}$  is the total auxin flux at the  $k$ th side of the cell. The total auxin flux is defined as the difference between outflux and influx. This model does not consider inter-cellular dynamics and assumes that auxin flows directly from one cell to the other.

The increasing function  $g(f_{ik})$  represents the PIN dependence on total auxin flux ( $f_{ik}$ ). It contains two other parameters, the flux sensitivity ( $\alpha$ ) and flux threshold ( $\beta$ ).  $f_0$  is fixed to  $B/A$  where  $B$  is the PIN synthesis rate.

If we initialize PIN concentrations with a rightward bias (see numerical calculations), this model can produce passage patterns observed in leaves. With “random bias” (see numerical calculations), the model can produce spot-like patterns (see figure 1), despite a claim by Hayakawa et al [4]. This model also does not take into consideration environmental stimuli. See discussion for further details.

### 4 Auxin Self-Feedback Model

Hayakawa et al. proposed an extension to the basic auxin flux model. Based on the assumption of a positive feedback effect between auxin concentration and

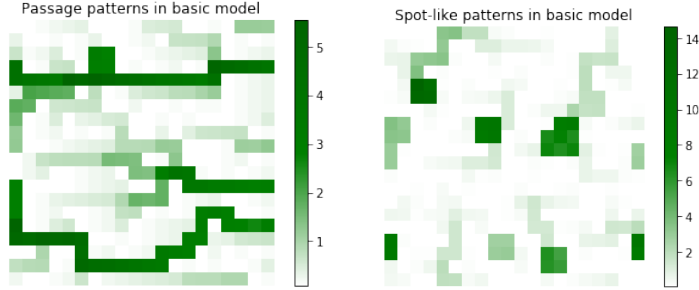


Figure 1: With initial directional bias (in this case, to the right by 10%), the system can generate passage like patterns (left) as observed in, for example, leaf veins. With a uniformly random PIN distribution, the system is also capable of producing spot-like patterns (right).

PIN from the basic auxin flux model, the group added a self-feedback effect for auxin synthesis in the rate of auxin concentration. This model works with the idea that if high-level concentrations of auxin increases its own levels autocatalytically, then there are more areas with high auxin concentration.

The equation for the rate of auxin concentration is replaced with,

$$\frac{da_i}{dt} = 1 + D \frac{a_i^n}{a_i^n + K_a} - Aa_i - \sum_k f_{ik}$$

where  $D$  is the strength of the auxin self-feedback,  $K_a$  is the threshold of the auxin self-feedback, and  $n$  is the Hill coefficient.

When  $A = 40$ ,  $D = 50$ , and the initial conditions have a random bias (parameter set 3, table 1), this model produces spot patterns (see figure 2). If  $A = 8$ ,  $D = 10$ , and the initial conditions are changed into one with a rightward bias (parameter set 2, table 1), the model produces passage patterns (see figure 2).

However, similar with Fujita et al.'s model, the auxin self-feedback model does not take into account environmental stimuli.

## 5 Model Extension

The basic auxin flux model assumes that auxin has constant rates of production and degradation proportional to auxin concentration at every cell. In the model,

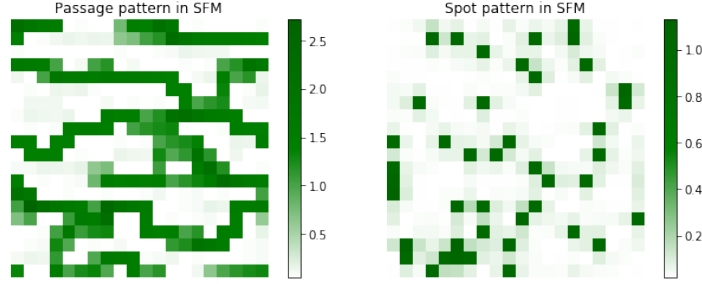


Figure 2: The self-feedback model (SFM) with different parameters. With the second parameter set (table 1), the system can generate passage like patterns (left) as observed in, for example, leaf veins. With parameter set 3 (table 1), the system is also capable of producing spot patterns (right).

each cell is initialized with auxin concentration  $\frac{1}{A}$  with additional noise from a random distribution  $\text{Unif}(-0.5, 0.5)$ .

This basic model is sufficient if we consider relatively short time scales. However, there are many external factors that contribute to auxin production. For example, heat and light affect auxin production ([2], [6], [12], [13]) and vary periodically on time scales from hours, days, and months.

As such, we propose that auxin production in each cell is able to be forced by some function  $\sigma(t)$ , which is a measure of some external factor in order to consider very long time behaviour.

The equation for the rate of auxin concentration in the basic auxin flux model is replaced with,

$$\frac{da_i}{dt} = \sigma(x) - Aa_i - \sum_k f_{ik}$$

While the equation for the rate of auxin concentration in the auxin self-feedback model is replaced with,

$$\frac{da_i}{dt} = \sigma(x) + D \frac{a_i^n}{a_i^n + K_a} - Aa_i - \sum_k f_{ik}$$

## 6 Discussion

### 6.1 Numerical Calculations

We simulated the system using a square geometry for the cells, as opposed to the hexagonal geometry imposed by [4] and [3]. That is, each cell has only four sides, arranged in a tight lattice.

Due to limited computational resources, simulations were run from  $t \in [0, 20]$  with only 100 steps. The system is solved by using the new `solve_ivp` module found in `SciPy 1.0.1` [5]. We let `solve_ivp` pick the solver, although the default is a Runge-Kutta method of order 5(4).

The lattice is a  $20 \times 20$  grid with periodic boundary conditions. That is, the right sides of the cells along the right edge are right next to the left side of the cells along the left edge, and similarly for the top and bottom edges.

Three sets of initial conditions are considered in this paper and found in table 1: Parameter set 1 is for the auxin-flux model (from [3]) and the other two are for the self-feedback model (from [4]).

	Parameter Set 1	Parameter Set 2	Parameter Set 3
$A$	1	8	40
$B$	10	10	10
$\alpha$	50	12	12
$\beta$	1	1	1
$f_0$	$B/A$	$B/A$	$B/A$
$n$	n/a	6	6
$D$	n/a	10	50
$K$	n/a	0.5	0.5
$a_i(0)$	Unbiased random	Unbiased random	Unbiased random
$p_i(0)$	Rightward bias	Rightward bias	$Y \sim \text{Unif}(0, 2)$

Table 1: Parameter sets used in this paper. Rightward bias is given by  $p_{ik}(0) = 1.1(B/6)$  if  $k$  is the right face,  $p_{ik}(0) = 0.9(B/6)$  if  $k$  is the left face, and  $p_{ik}(0) = B/6$  for the top and bottom face. Unbiased random is given by  $1 + X \sim \text{Unif}(-0.5, 0.5)$ , where  $X$  is a uniform random variable. Parameter set 1 is for the basic auxin-flux model. Parameter set 2 is used for generating passage patterns in the self-feedback model, and parameter set 3 is used for generating spot patterns in the self-feedback model.

### 6.2 Extended model results

For these results, we consider the sinusoidal forcing function

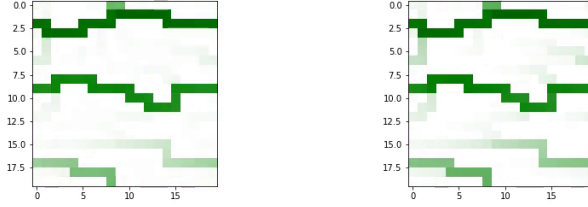


Figure 3: In the basic model with external forcing function  $\sigma(t)$ , we see that the two images at two consecutive troughs in  $\sigma(t)$  ( $t \approx 3\pi/2, 7\pi/2$ ) are nearly identical, indicating that auxin patterns are fairly robust.

$$\sigma(t) = \delta \sin(x) + \delta$$

### 6.2.1 Basic Model Extension

Using the first parameter set in table 1 along with the  $\sigma$  extension, we found that with  $\delta = 1$ , the main passages persist. By running a simulation (figure 3) and comparing the troughs in  $\sigma(t)$  (for which the main patterns are most dominant) we see that the main passages do not change.

This shows that auxin patterns in the basic model are fairly robust to fluctuations up to 100% of regular production rate.

### 6.2.2 Self-feedback Model Extension

Using the second parameter set in table 1 along with the  $\sigma$  extension, we found that with  $\delta = 1$ , the main passages persist. By running a simulation (figure 4) and comparing the troughs in  $\sigma(t)$  (for which the main patterns are most dominant) we see that the main passages do not change.

This shows that passage patterns in the self-feedback model are fairly robust to fluctuations up to 100% of regular production rate.

Using the third parameter set in table 1 along with the  $\sigma$  extension to generate spot patterns, we found that with  $\delta = 1$ , the spot patterns persist throughout fluctuations (figure 5). Furthermore, with the parameter set required to generate spot patterns (set 3, table 1), spot patterns are much less sensitive to production fluctuations than passage patterns (figure 6).

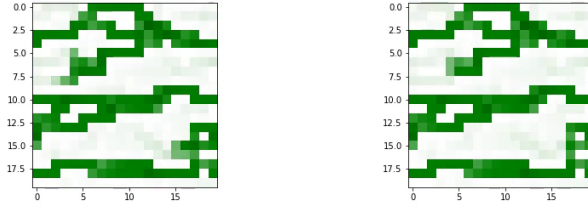


Figure 4: In the self-feedback model with external forcing function  $\sigma(t)$  and second parameter set in table 1, we see that the two images at two consecutive troughs in  $\sigma(t)$  ( $t \approx 3\pi/2, 7\pi/2$ ) are nearly identical, indicating that auxin patterns are fairly robust.

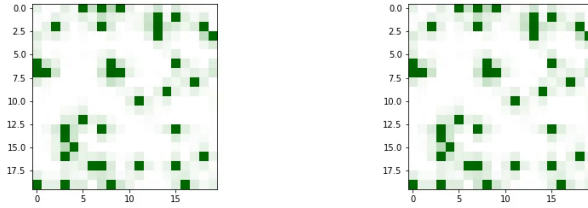


Figure 5: In the self-feedback model with external forcing function  $\sigma(t)$  and parameter set 3 (table 1), we see that the two images at two consecutive troughs in  $\sigma(t)$  ( $t \approx 3\pi/2, 7\pi/2$ ) are nearly identical, indicating that auxin patterns are fairly robust.

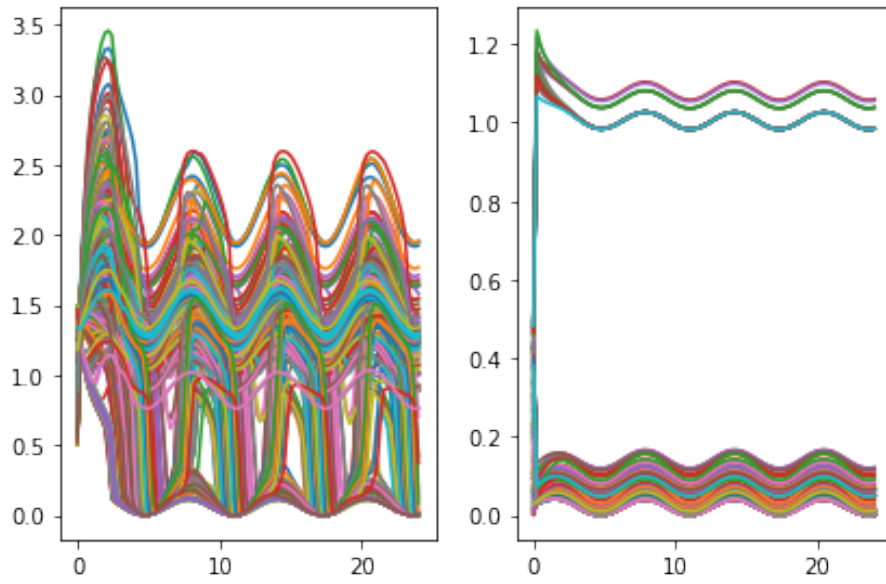


Figure 6: Time series of auxin concentrations of every cell for the passage patterns in the self-feedback model (left) and spot patterns (right). We see that despite identical forcing, the fluctuations are much less varied in the spot patterns.

### 6.3 High auxin production

In the basic and self feedback model, the equation describing auxin concentration looks like

$$\begin{aligned} \frac{da_i}{dt} &= 1 - Aa_i - \sum_k f_{ik} && \text{Basic model} \\ \frac{da_i}{dt} &= 1 + D \frac{a_i^n}{a_i^n + K_a} - Aa_i - \sum_k f_{ik} && \text{Self-feedback model} \end{aligned}$$

Instead of constant production 1, suppose we use a higher production rate, say 50. In fact, we see that if we use too high of a production rate, identifiable passage and spot patterns no longer appear (figure 7).

This is worth noting for those with commercial goals (for example, agriculture). In particular, it shows that simply modifying the auxin production pathway to only increase auxin production may not be fruitful, as without identifiable auxin patterns the plant may not grow as intended.

### 6.4 Spot-like patterns with the Basic Model

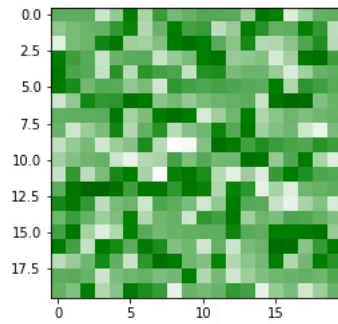
Using the parameter set

$$\begin{aligned} A &= 1 \\ B &= 10 \\ \alpha &= 50 \\ \beta &= 1 \\ f_0 &= B/A \\ a_i(0) &= 1 + X \sim \text{Unif}(-0.5, 0.5) \\ p_{ik}(0) &= (B/6) + Y \sim \text{Unif}(-0.1, 0.1) \end{aligned} \tag{1}$$

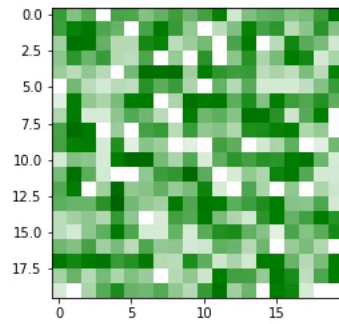
Which is similar to the first parameter set (table 1) aside from a uniformly random PIN, as opposed to a rightward bias in first parameter set.

Hayakawa et al. ([4]), using an approximation method they call the ‘Triplet Cell Approximation method’, determined that by searching the parameter space, that spot patterns were not possible from the basic auxin-flux model. However, as seen in figure 1 (right), ‘spot-like’ patterns do emerge.

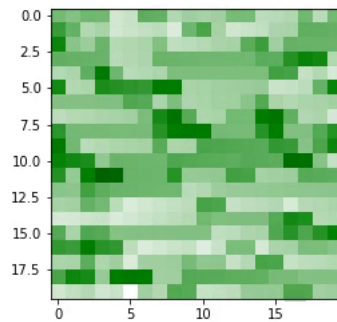
Evidently, comparing this with figure 5, the spots are much larger in ‘radius’. However, in shoot apical meristems, the areas of high auxin concentrations



(a)



(b)



(c)

Figure 7: Using a constant production rate of 50, we see that in the case of the self-feedback model with parameter set 2 (top left), self-feedback model with parameter set 3 (top right), and basic model with parameter set 1 (bottom), there are no identifiable spot or passage patterns.

where leaf or flower primordia would grow are closer to clusters of multiple cells, unlike singular isolated cells as in figure 5

This contradiction may be due to

- Geometry. In our model, we apply a square geometry to each cell whereas in [4], a hexagonal geometry is used. It may be the case that geometry plays a role in whether such patterns emerge.
- PIN is not the only factor that affects auxin concentration distribution. Different mechanisms, such as auxin interaction with multiple chemicals or defined pathways formed by other hormones present in plant tissues, might have a stronger effect on auxin spatial distribution.
- Inappropriate definitions. In [4], the authors scale down a large cell-lattice into a one-dimensional lattice (one row of three cells) with periodic boundary conditions that they call the ‘triplet cell approximation method’. With only  $3 + 3 * \text{numfaces}$  equations, the authors made concrete definitions for passage and spot patterns based on the smaller system. However, it may be possible that this definition does not accurately reflect in the larger system, and in real systems.

## 7 Conclusions

The resulting simulations of the basic model and the self-feedback model were able to produce both spot and passage patterns. Note however, the passage patterns in the basic model displayed lower maximum auxin concentrations compared to the spot patterns. The self-feedback model displays the opposite: the spot patterns are the ones with lower maximum auxin concentrations.

An interesting result appears in the simulations when the production rates of auxin are higher than [3] and [4]. The spot and passage patterns are “destroyed” and fail to persist or reform. The auxin concentration “floods” the plant tissue and a homogeneous spread of auxin is displayed.

Visually, the passage patterns in the basic model are more passage-like than the ones in the self-feedback model. The spot patterns in the basic model have larger area but occurred less frequently while the spot pattern in the self-feedback model have smaller area and occurred more. Similar results appear with our extension.

The results agree with biological intuition and current knowledge. Even though light and temperature affect the resulting auxin levels in plant tissue, the established patterns of auxins do not change. Leaf and flower primordia do not shift from where they sprout and leaf venation patterns do not change overnight. With our extension, the prominent steady-state passage and spot patterns displayed by both models persist throughout a wide range of  $\delta$  values. Therefore,

our extension to the models may provide further evidence for exploring the models. It also might be an indicator that such forcing functions contribute to the mechanisms that occur in actual plants.

However, similar to both models presented, our proposed extension lacks experimental data for confirmation. Furthermore, there are other external and internal factors besides light and temperature whose effects on auxin are not fully explored yet. Our model is limited due to how complex the relationships between these other factors and auxin production. Other mathematical models exist for intracellular auxin behaviour in plant tissues under different assumptions. Examples include taking into consideration a dynamically growing tissue and the effects of structural changes to auxin production [10] and exploring the interaction between auxin and other plant hormones such as cytokinin. A unified general model could be assembled by integrating ideas from current existing mathematical models, including a forcing function that represents periodic external stimuli, similar to the one presented in this paper. This general model, in theory, could accurately predict the resulting auxin pattern, given a set of physical and biochemical parameters.

## References

- [1] René Benjamins and Ben Scheres. “Auxin: The Looping Star in Plant Development”. In: *Annual Review of Plant Biology* 59.1 (2008). PMID: 18444904, pp. 443–465. DOI: 10.1146/annurev.arplant.58.032806.103805. eprint: <https://doi.org/10.1146/annurev.arplant.58.032806.103805>. URL: <https://doi.org/10.1146/annurev.arplant.58.032806.103805>.
- [2] Keara A. Franklin et al. “Interaction of light and temperature signalling”. In: *Journal of Experimental Botany* 65.11 (2014), pp. 2859–2871. DOI: 10.1093/jxb/eru059. URL: <http://dx.doi.org/10.1093/jxb/eru059>.
- [3] Hironori Fujita and Atsushi Mochizuki. “The origin of the diversity of leaf venation pattern”. In: *Developmental Dynamics* 235.10 (), pp. 2710–2721. DOI: 10.1002/dvdy.20908. eprint: <https://onlinelibrary.wiley.com/doi/pdf/10.1002/dvdy.20908>. URL: <https://onlinelibrary.wiley.com/doi/abs/10.1002/dvdy.20908>.
- [4] Yoshinori Hayakawa, Masashi Tachikawa, and Atsushi Mochizuki. “Mathematical study for the mechanism of vascular and spot patterns by auxin and pin dynamics in plant development”. In: *Journal of Theoretical Biology* 365 (2015), pp. 12–22. ISSN: 0022-5193. DOI: <https://doi.org/10.1016/j.jtbi.2014.09.039>. URL: <http://www.sciencedirect.com/science/article/pii/S0022519314005864>.
- [5] Eric Jones, Travis Oliphant, Pearu Peterson, et al. *SciPy: Open source scientific tools for Python*. 2001–. URL: <http://www.scipy.org/>.

- [6] Martina Legris et al. “Perception and signalling of light and temperature cues in plants”. In: *The Plant Journal* 90.4 (), pp. 683–697. DOI: 10.1111/tpj.13467. URL: <https://onlinelibrary.wiley.com/doi/abs/10.1111/tpj.13467>.
- [7] Jan Petrášek and Jiří Friml. “Auxin transport routes in plant development”. In: *Development* 136.16 (2009), pp. 2675–2688. ISSN: 0950-1991. DOI: 10.1242/dev.030353. eprint: <http://dev.biologists.org/content/136/16/2675.full.pdf>. URL: <http://dev.biologists.org/content/136/16/2675>.
- [8] Didier Reinhardt et al. “Regulation of phyllotaxis by polar auxin transport”. In: *Nature* 426 (Nov. 2003). Article, p. 255. URL: <http://dx.doi.org/10.1038/nature02081>.
- [9] Tsvi Sachs. “The Control of the Patterned Differentiation of Vascular Tissues”. In: *Advances in Botanical Research*. Elsevier, 1981, pp. 151–262. DOI: 10.1016/s0065-2296(08)60351-1. URL: [https://doi.org/10.1016/s0065-2296\(08\)60351-1](https://doi.org/10.1016/s0065-2296(08)60351-1).
- [10] Massimiliano Sassi et al. “An Auxin-Mediated Shift toward Growth Isotropy Promotes Organ Formation at the Shoot Meristem in Arabidopsis”. In: *Current Biology* 24.19 (Oct. 2014), pp. 2335–2342. DOI: 10.1016/j.cub.2014.08.036. URL: <https://doi.org/10.1016/j.cub.2014.08.036>.
- [11] E. Scarpella. “Control of leaf vascular patterning by polar auxin transport”. In: *Genes Development* 20.8 (Apr. 2006), pp. 1015–1027. DOI: 10.1101/gad.1402406. URL: <http://dx.doi.org/10.1101/gad.1402406>.
- [12] Elin Thingnaes et al. “Day and Night Temperature Responses in Arabidopsis: Effects on Gibberellin and Auxin Content, Cell Size, Morphology and Flowering Time”. In: *Annals of Botany* 92.4 (Oct. 2003), pp. 601–612. DOI: 10.1093/aob/mcg176. URL: <https://doi.org/10.1093/aob/mcg176>.
- [13] Mieke de Wit, Séverine Lorrain, and Christian Fankhauser. “Auxin-mediated plant architectural changes in response to shade and high temperature”. In: *Physiologia Plantarum* 151.1 (2013), pp. 13–24. DOI: 10.1111/ppl.12099. URL: <https://onlinelibrary.wiley.com/doi/abs/10.1111/ppl.12099>.